

## Optimized Recording of Heteronuclear Multidimensional NMR Spectra Using Pulsed Field Gradients

AD BAX\* AND SUSAN S. POCHAPSKY†

\*Laboratory of Chemical Physics, National Institutes of Diabetes and Digestive and Kidney Diseases, National Institutes of Health, Bethesda, Maryland 20892; and †Bruker Instruments, Inc., Manning Park, Billerica, Massachusetts 01821

Received June 29, 1992

Many of the recently introduced triple-resonance experiments (1-7) are of high intrinsic sensitivity and frequently the minimum time needed for recording such spectra is dictated by the required digital resolution and by the number of phase-cycling steps needed for artifact suppression. Recently, it has been convincingly demonstrated that effective suppression of artifacts and selection of a desired coherence-transfer pathway can be accomplished by using pulsed field gradients (PFG) (8-14). Although all the earlier methods relied on detection of phase-modulated signals, requiring absolute-value-mode processing, recently it has been shown possible to record absorption-mode spectra using PFG techniques (13, 14). Unfortunately, both the absolute-value-mode PFG schemes and the PFG methods that yield pure absorptive lineshapes have an inherent sensitivity lower than that of their phase-cycled analogs. This lower sensitivity is related to the fact that in all these experiments the pulsed field gradient is used to select a desired coherence-transfer pathway and it is not possible to simultaneously select both coherence of level  $n$  and level  $-n$ . The so-called SWAT experiment (15), using rapidly switching field gradients during data acquisition, is an exception to this rule, but this experiment requires an audiofrequency bandwidth much wider than the width of the sampled spectral window, decreasing sensitivity even more.

Here we describe the use of a number of pulse-sequence elements that utilize pulsed field gradients and that do not suffer from the disadvantages mentioned above. Although these individual elements have been known for many years, it has not been recognized that in many applications the gradients provide sufficient artifact suppression to remove the need for phase cycling altogether. The basic philosophy behind the design of these elements is to keep all desired magnetization-transfer pathways intact and to insert gradient pulses only when this can be done without affecting the intrinsic sensitivity of the experiment.

Most heteronuclear experiments consist of a number of common "building blocks." Three of these are discussed below, together with their pulsed-field-gradient versions.

**Heteronuclear magnetization transfer.** Magnetization transfer between two  $J$ -coupled heteronuclei, I and S, is frequently accomplished by a pair of  $90^\circ$  pulses, preceded and followed by delays for  $J$  dephasing and rephasing. Usually the two  $90^\circ$  pulses are applied simultaneously, but this need not be the case, and delays that are much shorter

than the  $T_1$  of the coupled nuclei may be inserted without significantly affecting the sensitivity of the experiment. In terms of the product-operator formalism, the desired magnetization transfer goes as follows:

$$I_x S_z \xrightarrow{90_y^\circ(I)} -I_z S_z \xrightarrow{90_y^\circ(S)} -I_z S_x. \quad [1a]$$

Unwanted magnetization is associated with terms such as

$$I_y S_z \xrightarrow{90_y^\circ(I)} I_y S_z \xrightarrow{90_y^\circ(S)} I_y S_x \quad [1b]$$

$$I_y \xrightarrow{90_y^\circ(I)} I_y \xrightarrow{90_y^\circ(S)} I_y \quad [1c]$$

or

$$I_x \xrightarrow{90_y^\circ(I)} -I_z \xrightarrow{90_y^\circ(S)} -I_z. \quad [1d]$$

If the PFG is applied between the two  $90^\circ$  pulses (Fig. 1a), it is clear that only terms which are longitudinal after the  $90_y^\circ(I)$  pulse are retained, and the terms in [1b] and [1c] are effectively defocused. However, unwanted magnetization of [1d] is not affected by the PFG and must be eliminated by an RF scrambling pulse (16, 17) (*vide infra*).

**$180^\circ$  refocusing pulse.** Whenever a refocusing pulse is applied to a single-spin species (e.g.,  $S$ ), this provides the opportunity to select terms that have a transverse spin operator ( $S_x$  or  $S_y$ ) both before and after the pulse. This is accomplished by applying two gradient pulses of equal strength and polarity before and after the  $180^\circ$  pulse (Fig. 1b). These gradient pulses eliminate the effect of pulse imperfections which may transfer, for example,  $S_x$  to  $S_z$  or  $S_z$  to  $S_x$ . In addition, any transverse operator for spins which do not experience the  $180^\circ$  pulse is effectively defocused.

**$180^\circ$  decoupling pulse.** Many of the heteronuclear pulse schemes include so-called  $180^\circ$  heteronuclear decoupling pulses which serve to invert the spin state of a heteronucleus, represented by  $I_z$  or  $S_z$ . By applying two field-gradient pulses of equal strength but opposite polarity before and after this  $180^\circ$  decoupling pulse (Fig. 1c), the effect of any  $180^\circ$  pulse imperfection, which would result in  $z$  operators being transformed to transverse spin operators, is eliminated.

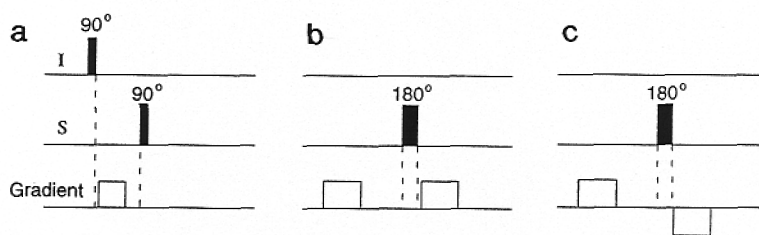


FIG. 1. Examples of different applications of pulsed field gradients in heteronuclear NMR. (a) Selection of an  $I_z S_z$  intermediate, (b) selection of transverse  $S$ -spin magnetization which is being refocused by a  $180^\circ$  pulse, and (c) elimination of transverse  $S$ -spin components caused by an imperfect  $180^\circ$  ( $S$ ) decoupling pulse.

Examples of all three applications of gradient pulses mentioned above are illustrated for the constant-time CT-HN(CO)CA experiment (4), in which magnetization from an amide proton is transferred to its attached  $^{15}\text{N}$  and then relayed via the  $^{13}\text{CO}$  nucleus to the  $\text{C}_\alpha$  of the preceding amino acid, followed by the reverse pathway for  $^1\text{H}$  detection. The pulse scheme is sketched in Fig. 2. Its mechanism has been described previously (3, 4) and will not be repeated here. The first gradient pulse,  $G_1$ , serves to eliminate any terms that are not longitudinal in the  $^1\text{H} \rightarrow ^{15}\text{N}$  magnetization-transfer process and is an example of the use of the element shown in Fig. 1a.  $G_1$  eliminates the need for the usual  $\pm y$  phase cycle of the  $90^\circ$   $^1\text{H}$  pulse, commonly used for this purpose. The pair of gradient pulses,  $G_2$ , eliminates magnetization that is not refocused by the  $180^\circ$   $^{15}\text{N}$  pulse, applied between the two  $G_2$  pulses, and is an example of the use of the element shown in Fig. 1b. The  $G_2$  gradient pulses must be sufficiently strong to dephase (and rephase)  $^{15}\text{N}$  magnetization, which takes  $\gamma_{\text{H}}/\gamma_{\text{N}} \approx 10$  times longer than that for  $^1\text{H}$  magnetization. The  $G_2$  pulses eliminate the need for the usual four-step phase cycle of the  $180^\circ$   $^{15}\text{N}$  pulse. The  $G_3$  pulses are of the same type (Fig. 1b) as  $G_2$  and serve to eliminate effects caused by imperfections of the  $180^\circ$  pulse in the middle of the  $180^\circ$   $t_2$  period and, more importantly, to dephase any transverse  $^{15}\text{N}$  spin operators. This latter function previously was obtained by a  $\pm x$  phase cycle of the  $90^\circ$   $^{15}\text{N}$  pulse immediately preceding the  $\epsilon$  dephasing delay (3, 4).

Gradient pulses  $G_4$  are of opposite relative polarity and are of the type shown in Fig. 1c. They eliminate any transverse magnetization generated by the (imperfect)  $180^\circ$  ( $^1\text{H}$ ) decoupling pulse which they surround. Finally, the  $G_5$  pulses ensure that

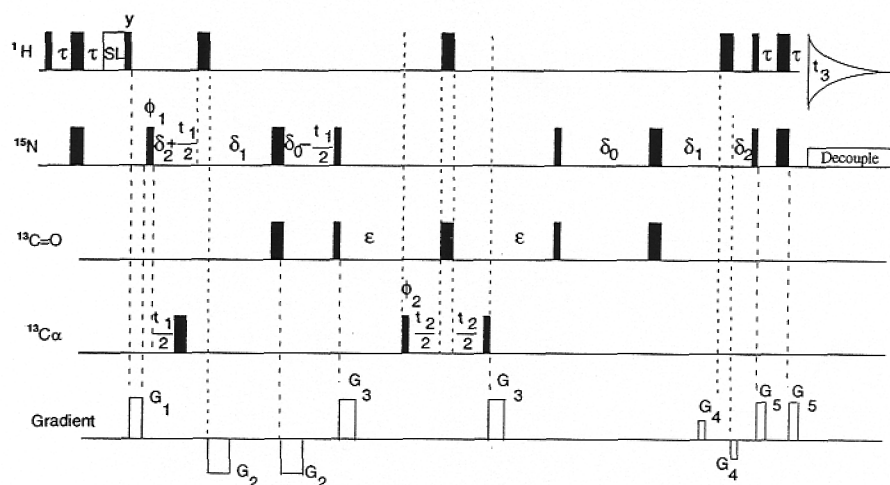


FIG. 2. Pulse scheme of the 3D CT-HN(CO)CA experiment. All pulses, unless explicitly indicated, are applied along the  $x$  axis. The spin-lock pulse, SL, has a duration of 1 ms and an RF field strength of 25 kHz. The phases of the  $90^\circ_{\phi_1}$  and  $90^\circ_{\phi_2}$  pulses are changed in the regular States-TPPI manner (18) to obtain quadrature in the  $t_1$  and  $t_2$  dimensions, respectively. All gradient pulses except  $G_4$  (3.5 G/cm) are applied using a gradient strength of  $\sim 9$  G/cm. The durations of the PFGs are as follows:  $G_1$ , 150  $\mu\text{s}$ ;  $G_2$ , 1.5 ms;  $G_3$ , 450  $\mu\text{s}$ ;  $G_4$ , 100  $\mu\text{s}$ ;  $G_5$ , 150  $\mu\text{s}$ . For reasons of convenience, all PFGs were of rectangular shape. Durations of the various delays are as follows:  $\tau$  = 2.25 ms;  $\delta_0$  = 12 ms;  $\delta_1$  = 9.25 ms;  $\delta_2$  = 2.75 ms;  $\epsilon$  = 6.6 ms. Spectral widths used are 32.9 ppm ( $F_1$ ,  $^{15}\text{N}$ ); 33.1 ppm ( $F_2$ ,  $^{13}\text{C}_\alpha$ ); 16.1 ppm ( $F_3$ ,  $^1\text{H}$ ).

the magnetization detected during the acquisition period stems from single-quantum  $^1\text{H}$  coherence which must be present during both the final  $\tau$  periods, eliminating the possibility for spurious  $^1\text{H}$ - $^{15}\text{N}$  multiple-quantum coherence present before the last pair of  $180^\circ$  pulses to be transformed into observable signals. Provided RF pulse widths have been carefully calibrated, the artifacts suppressed by the gradient pulses  $G_4$  and  $G_5$  are usually quite weak. Consequently, in phase-cycled experiments usually no phase-cycling steps are dedicated to their removal.

As mentioned above, spurious terms of the type in Eq. [1d] remain longitudinal during the entire pulse sequence until the final  $^1\text{H}$   $90^\circ$  pulse transforms them into observable signal. These terms do not show  $t_1$  or  $t_2$  modulation and result in the well-known axial peaks, which fall at the edge of the spectrum in the  $F_1$  and  $F_2$  dimension if either the TPPI (18) or the States-TPPI (19) method is used to obtain quadrature in the  $t_1$  and  $t_2$  dimensions. Their intensity can be strongly attenuated by using a "scrambling pulse" (16, 17), labeled SL, prior to the first INEPT transfer. This pulse spin locks the antiphase  $^1\text{H}\{-^{15}\text{N}\}$  doublet components, and any magnetization perpendicular to this spin-lock field is scrambled by RF inhomogeneity. In the CT-HN(CO)CA experiment, there is a second source of magnetization which contributes to spurious axial peaks: A fraction,  $\cos^2(\pi J_{\text{COCA}}\epsilon)$ , of carbonyl magnetization does not follow the  $^{13}\text{CO}$ - $^{13}\text{C}_\alpha$  multiple-quantum path during  $t_2$  and shows zero modulation in this dimension, resulting in relatively weak axial peaks.

One final point which requires careful consideration relates to the polarity of the gradient pulses. If multiple gradients are used, it is necessary to ensure that their effects are additive to the largest possible extent, eliminating the need for using very strong gradient pulses. As a  $180^\circ$  ( $^1\text{H}$ ) pulse separates  $G_1$  and the two  $G_2$  pulses, the preferred polarity of  $G_2$  is opposite to  $G_1$ , i.e., negative. The two  $G_3$  pulses are separated by a  $^1\text{H}$   $180^\circ$  pulse and their polarity is arbitrarily chosen positive. Because the first  $G_4$  pulse is separated from  $G_2$  by a  $180^\circ$   $^1\text{H}$  pulse its polarity must be opposite to  $G_2$ , i.e., positive. The  $G_5$  pulses are separated from the preceding gradient pulses by a  $90^\circ$   $^1\text{H}$  pulse, and their polarity is arbitrarily chosen positive.

The experiment is demonstrated for a 1.5 mM sample of uniformly ( $>95\%$ )  $^{13}\text{C}$ / $^{15}\text{N}$ -enriched calmodulin, complexed with a 26-residue peptide, dissolved in 95%  $\text{H}_2\text{O}$ /10%  $\text{D}_2\text{O}$ , pH 6.95. Total mass of this globular complex (20) is 19.7 kDa. Experiments were carried out on a Bruker AMX-500 spectrometer, equipped with a Bruker gradient accessory and triple-resonance probehead with a self-shielded  $z$ -gradient coil. No  $\text{H}_2\text{O}$  presaturation was used, and data were processed with standard Bruker software.

Figure 3 shows two  $^1\text{H}$ - $^{13}\text{C}_\alpha$  planes of a 3D CT-HN(CO)CA spectrum recorded without phase cycling in a total measuring time of 1.74 hours, using a  $32^*(t_1, ^{15}\text{N}) \times 46^*(t_2, ^{13}\text{C}_\alpha) \times 512^*(t_3, \text{H}_\text{N})$  data matrix. The same slices of the 3D spectrum of this protein-peptide complex, recorded in 40 hours at 600 MHz  $^1\text{H}$  frequency, have been shown previously (3). Although the signal-to-noise ratio of the present 3D spectrum is clearly lower than that in the earlier work (due to the shorter measuring time and the lower field strength), all resonances previously observed are visible in the present spectrum.

Our results show that a dramatic reduction or complete removal of the lengthy phase-cycling procedure typically used in heteronuclear multidimensional experiments is possible without any adverse effects on lineshape or sensitivity [apart from a possibly



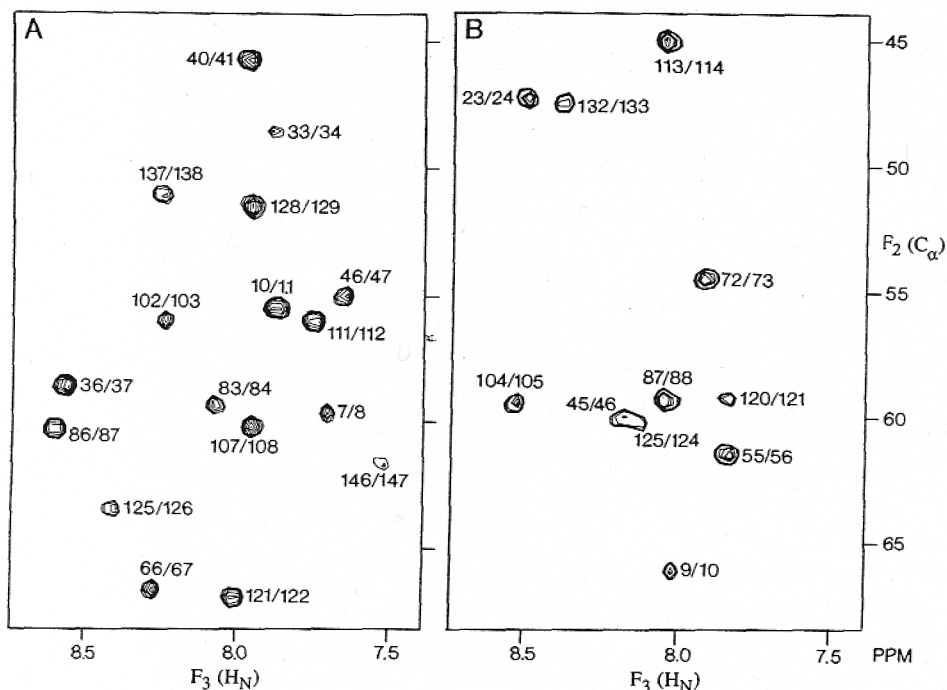


FIG. 3. Two ( $F_2$ ,  $F_3$ ) slices from the CT-HN(CO)CA spectrum, taken at  $^{15}\text{N}$  chemical shifts ( $F_1$ ) of (A) 121 and (B) 118 ppm. Corresponding slices obtained with a phase-cycled version of the HN(CO)CA experiment are given in Ref. (3). The spectrum was recorded in 1.75 hours and processed using 60°-shifted sine-bell apodization in the  $t_1$  and  $t_2$  dimensions and 60°-shifted squared-sine-bell filtering in the  $t_3$  dimension. The matrix was zero filled to yield a  $256 \times 128 \times 1024$  matrix for the absorptive part of the final 3D spectrum. Because of the constant-time nature of the  $^{15}\text{N}$  evolution period, the resolution in the  $^{15}\text{N}$  dimension is slightly higher than that in the previous work (3), causing the 81/82 correlation (Glu82  $^{15}\text{N}$ , 121.6 ppm) to be absent in (A). This "missing" correlation is clearly observed in the  $F_1 = 121.6$  ppm slice, however.

slightly lower ( $\sim 10$ – $20\%$ ) sensitivity for a gradient probe compared to a standard probe]. In fact, a comparison of the performance of the scheme shown in Fig. 2, using the phase-cycling scheme of Grzesiek and Bax (4) in the absence and presence of pulsed field gradients, indicated that the gradients do not result in any notable signal loss. Note, however, that the pulsed field gradients in our present work are relatively small compared to those in most previous studies, decreasing the effects that any imperfections or instabilities of gradient pulses might cause. The field gradients in the scheme of Fig. 2 increase the water suppression by  $\sim 10$ -fold over the  $\sim 20$ -fold suppression obtained with the water purge pulse, SL. Although this degree of suppression is more than what is typically obtained by simple presaturation of the  $\text{H}_2\text{O}$  resonance, the residual water signal causes the usual  $t_1$  noise close to the  $F_3$   $\text{H}_2\text{O}$  frequency. Note that much higher degrees of water suppression are obtainable by using the previously published coherence pathway selection schemes, combined with the use of very strong gradients (11). However, for the reasons discussed above, such experiments suffer from lower inherent sensitivity. For the application of heteronuclear experiments

to isotopically labeled compounds, where the artifacts to be suppressed by phase cycling frequently are not much stronger than the resonances of interest, the simple elements discussed above provide sufficient suppression without any loss in sensitivity.

## ACKNOWLEDGMENTS

We thank Clemens Anklin for useful advice and Geerten Vuister for stimulating discussions. This work was supported by the AIDS Targeted Anti-Viral Program of the Office of the Director of the National Institutes of Health.

## REFERENCES

1. M. IKURA, L. E. KAY, AND A. BAX, *Biochemistry* **29**, 4659 (1990).
2. L. E. KAY, M. IKURA, R. TSCHUDIN, AND A. BAX, *J. Magn. Reson.* **89**, 596 (1990).
3. A. BAX AND M. IKURA, *J. Biomol. NMR* **1**, 99 (1991).
4. S. GRZESIEK AND A. BAX, *J. Magn. Reson.* **96**, 432 (1992).
5. R. T. CLUBB, V. THANABAL, AND G. WAGNER, *J. Magn. Reson.* **97**, 213 (1992).
6. S. GRZESIEK AND A. BAX, *J. Am. Chem. Soc.*, in press.
7. A. G. PALMER III, W. J. FAIRBROTHER, J. CAVANAGH, P. E. WRIGHT, AND M. RANCE, *J. Biomol. NMR* **2**, 103 (1992).
8. A. BAX, P. G. DE JONG, A. F. MEHLKOPF, AND J. SMIDT, *Chem. Phys. Lett.* **69**, 567 (1980).
9. P. BARKER AND R. FREEMAN, *J. Magn. Reson.* **64**, 334 (1985).
10. R. E. HURD AND B. K. JOHN, *J. Magn. Reson.* **91**, 648 (1991).
11. B. K. JOHN, D. PLANT, S. L. HEALD, AND R. E. HURD, *J. Magn. Reson.* **94**, 664 (1991).
12. G. W. VUISTER, R. BOELEN, R. KAPTEIN, R. E. HURD, B. JOHN, AND P. C. M. VAN ZIJL, *J. Am. Chem. Soc.* **113**, 9688 (1991).
13. A. L. DAVIS, E. D. LAUE, J. KEELER, D. MOSKAU, AND J. LOHMAN, *J. Magn. Reson.* **94**, 637 (1991).
14. A. L. DAVIS, R. BOELEN, AND R. KAPTEIN, *J. Biomol. NMR*, in press.
15. R. E. HURD, B. K. JOHN, AND H. D. PLANT, *J. Magn. Reson.* **93**, 666 (1991).
16. C. J. R. COUNSELL, M. H. LEVITT, AND R. R. ERNST, *J. Magn. Reson.* **64**, 470 (1985).
17. B. A. MESSERLE, G. WIDER, G. OTTING, C. WEBER, AND K. WÜTHRICH, *J. Magn. Reson.* **85**, 608 (1989).
18. D. MARION AND K. WÜTHRICH, *Biochem. Biophys. Res. Commun.* **113**, 967 (1983).
19. D. MARION, M. IKURA, R. TSCHUDIN, AND A. BAX, *J. Magn. Reson.* **85**, 393 (1989).
20. M. IKURA, G. M. CLORE, A. M. GRONENBRON, G. ZHU, C. B. KLEE, AND A. BAX, *Science* **256**, 632 (1992).